Supplementary Figure 1: Δ9-THC induces ESCs proliferation for as low as 1nM.
(A) Whisker boxplot indicating the median cellular viability of ESCs exposed to the different Δ9-THC doses and associated errors. **(B)** Whisker boxplot indicating the median number of viable cells exposed to the different Δ9-THC doses indicated and associated errors. At least three independent biological repeats with three technical replicates (N=3, n=3). Statistical significance: *(p<0.05), ***(p<0.001), ****(p<0.0001).

Supplementary Figure 2: Δ9-THC induces alteration in ESCs cell cycle.
(A) Representative flow contour plots showing distribution of BrdU-stained and DAPI-stained cells, exposed to the different doses of Δ9-THC indicated. The frequency of events in each gate is indicated. **(B)** The median percentage of events and associated errors for each cell cycle gate were plotted in histograms. At least three independent biological repeats with three technical replicates (N=3, n=3). Statistical significance: *(p<0.05), **(p<0.01).

Supplementary Figure 3: Δ9-THC exposure in male ESCs also provokes cell proliferation.
(A) Whisker boxplot indicating the median cellular viability of male ESCs (the R8 cell line, see Material and Methods section) exposed to the different Δ9-THC doses and associated errors. **(B)** Whisker boxplot indicating the median number of viable cells exposed to the different Δ9-THC doses indicated and associated errors. At least three independent biological repeats with three technical replicates (N=3, n=3). Statistical significance: *(p<0.05), **(p<0.01), ****(p<0.0001).

Supplementary Figure 4: hESCs cell number decreases upon Δ9-THC exposure.
(A) Whisker boxplot indicating the median cellular viability of human embryonic stem cells continuously exposed to 100nM Δ9-THC doses over 6 days and associated errors. **(B)** Whisker boxplot indicating the median number of viable cells exposed to 100nM of Δ9-THC doses indicated and associated errors. For (A and B), 6 technical repeats of 2 biological repeats (n=12) were plotted. Statistical significance: **(p<0.01).

Supplementary Figure 5: hESCS metabolism is slightly but significantly impacted by Δ9-THC exposure.
The NAD(P)+/NADPH ratio of hESCs exposed to 100nM of Δ9-THC was normalized to the one measured in the mock-treated condition. Median and associated errors were plotted in whisker boxplots. One representative experiment out of two independent experiments was used to plot results. Statistical significance: *(p<0.05).

Supplementary Figure 6: Extracellular acidification rates and oxygen consumption rates in ESCs and EpiLCs upon Δ9-THC exposure.
(A and B) Traces were plotted for the extracellular acidification rate (ECAR) measurements in ESCs and EpiLCs, respectively, exposed to the different Δ9-THC doses indicated and normalized to the protein content. The oligomycin injection time is indicated by an arrow and allows to differentiate basal glycolytic rate from maximal glycolytic rate (when mitochondria are inhibited). The datapoints used in the main figure correspond to the first timepoint in the maximal glycolytic capacity section. **(C and D)** Traces were plotted for the oxygen consumption rate (OCR) measurements in ESCs and EpiLCs, respectively, exposed to the different Δ9-THC doses indicated and normalized to the protein content. The oligomycin, FCCP and AntimycinA/Rotenone injection times are indicated by arrows and allow to differentiate basal respiration from ATP-coupled respiration and maximal respiratory capacity. The datapoints used in the main figure correspond to the second timepoint in the maximal respiratory capacity section. FCCP: Carbonyl cyanide-p-trifluoromethoxyphenylhydrazone. Statistical significance: *(p<0.05), **(p<0.01), ****(p<0.0001).

Supplementary Figure 7: Metabolite profiling in ESCs and EpiLCs upon Δ9-THC exposure.
(A and B) Heatmaps showing the log2 of the amount of each metabolite upregulated in ESCs and EpiLCs upon exposure to 100nM of Δ9-THC. The relative amounts of metabolites were normalized to the mean value across all samples for one same condition and to the number of viable cells harvested in parallel on a control plate. **(C)** Histograms showing the ratio of reduced to oxidized glutathione (GSH/GSSG) based on the amounts measured in the metabolomics profiling.

Supplementary Figure 8: Extracellular acidification rates and oxygen consumption rates in ESCs upon Δ9-THC and 2-DG exposure.
(A) Traces were plotted for the extracellular acidification rate (ECAR) measurements in ESCs exposed to 100nM of Δ9-THC and 10mM of 2-DG, as indicated, and normalized to the protein content. The oligomycin injection time is indicated by an arrow and allows to differentiate basal glycolytic rate from maximal glycolytic rate (when mitochondria are inhibited). **(B)** Traces were plotted for the oxygen consumption rate (OCR) measurements in ESCs exposed to 100nM of Δ9-THC and 10mM of 2-DG, as indicated, and normalized to the protein content. The oligomycin, FCCP and AntimycinA/Rotenone injection times are indicated by arrows and allow to differentiate basal respiration from ATP-coupled respiration and maximal respiratory capacity. FCCP: Carbonyl cyanide-p-trifluoromethoxyphenylhydrazone. Statistical significance: *(p<0.05), **(p<0.01).

Supplementary Figure 9: Δ9-THC exposure does not alter markers of pluripotency.
Gene expression profiles of markers for the inner cell mass (ICM) and epiblast. Histograms show the median and associated errors of normalized gene counts in each condition, as indicated.

Supplementary Figure 10: Δ9-THC exposure alter the expression of some epigenetic modifiers.
Histograms show the median and associated errors of normalized gene counts in each condition, as indicated. Only genes with |(log2(FC)|>0.25 and p-value<0.01 from Supplementary Table 1 were plotted. Statistical significance: **(p<0.01), ***(p<0.001), ****(p<0.0001).

Supplementary Figure 11: PGCLCs gating and sorting strategy.
(A) Representative flow contour plots showing distribution of events and gating based on embryoid bodies dissociation. **(B and C)** Representative flow contour plots to isolate singlets based on width to height ratios on the side scatter and front scatter, respectively. **(D)** Gating strategy for Stella:CFP versus Blimp1:mVenus on the negative control, corresponding to embryoid bodies obtained in an induction medium without cytokines and BMPs (GK15 only). **(E)** Gating strategy for Stella:CFP versus Blimp1:mVenus on mock-treated cells, corresponding to embryoid bodies obtained in an induction medium complemented with cytokines and BMPs. DN: double negative, SP: single positive, DP: double positive subpopulations.

Supplementary Figure 12: Male PGCLCs deriving from ESCs and EpiLCs exposed to 100nM of Δ9-THC proliferate.
(A) Diagram illustrating Δ9-THC exposure scheme and experimental strategy. **(B)** Representative flow contour plots showing distribution of live-gated events, gating strategy for Stella:CFP versus Blimp1:mVenus and percentages of cells in each subpopulations for ESCs and EpiLCs exposed to 100nM of Δ9-THC. DN: double negative, SP: single positive, DP: double positive subpopulations. **(C)** The percentage of events in the gates associated to each subpopulation was normalized to the one measured in the mock-treated condition. Median and associated errors were plotted in whisker boxplots independently for each subpopulation. At least three independent biological repeats with three technical replicates (N=3, n=3). Statistical significance: *(p<0.05).

Supplementary Figure 13: No residual Δ9-THC is detected in day 5 embryoid bodies.
Intracellular levels of Δ9-THC were quantified by mass spectrometry in EpiLCs on the day of aggregate formation and in day 5 embryoid bodies (referred as to “EpiLCs” and “PGCLCs”). Histograms show the median and associated errors of two independent quantifications. Statistical significance: ****(p<0.0001).

SUPPLEMENTARY FIGURES

Supplementary Figure 1

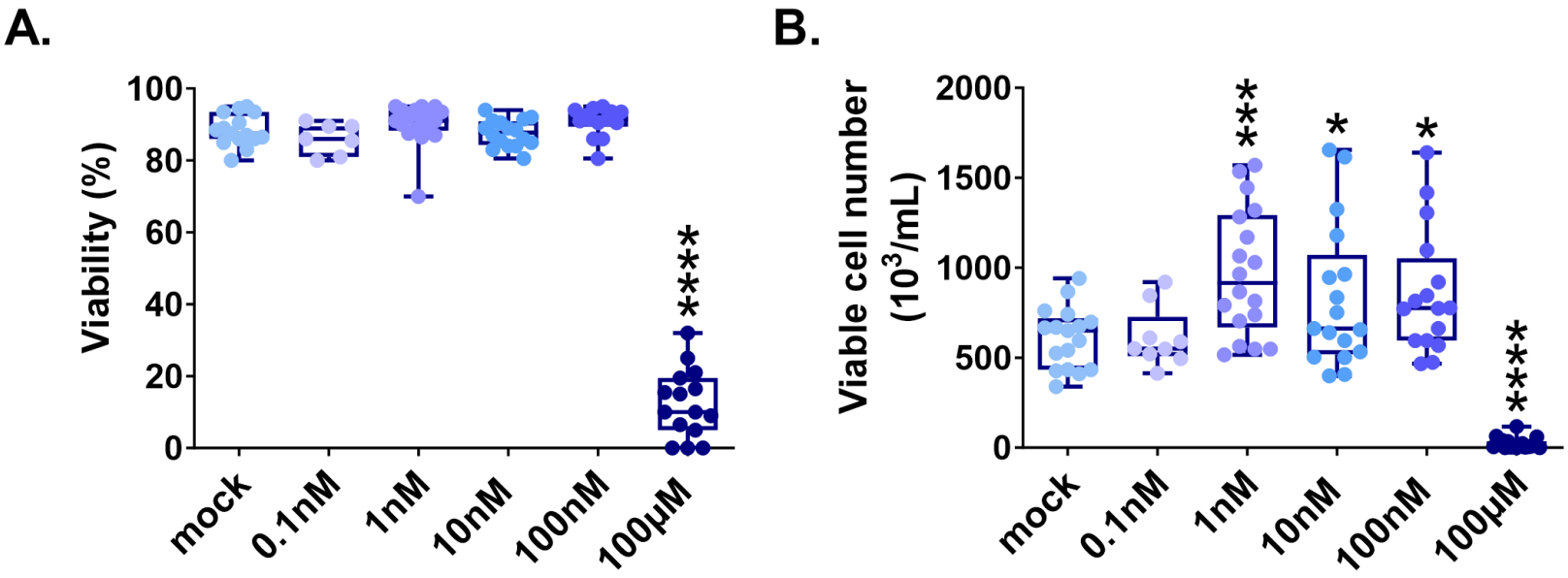

Supplementary Figure 2

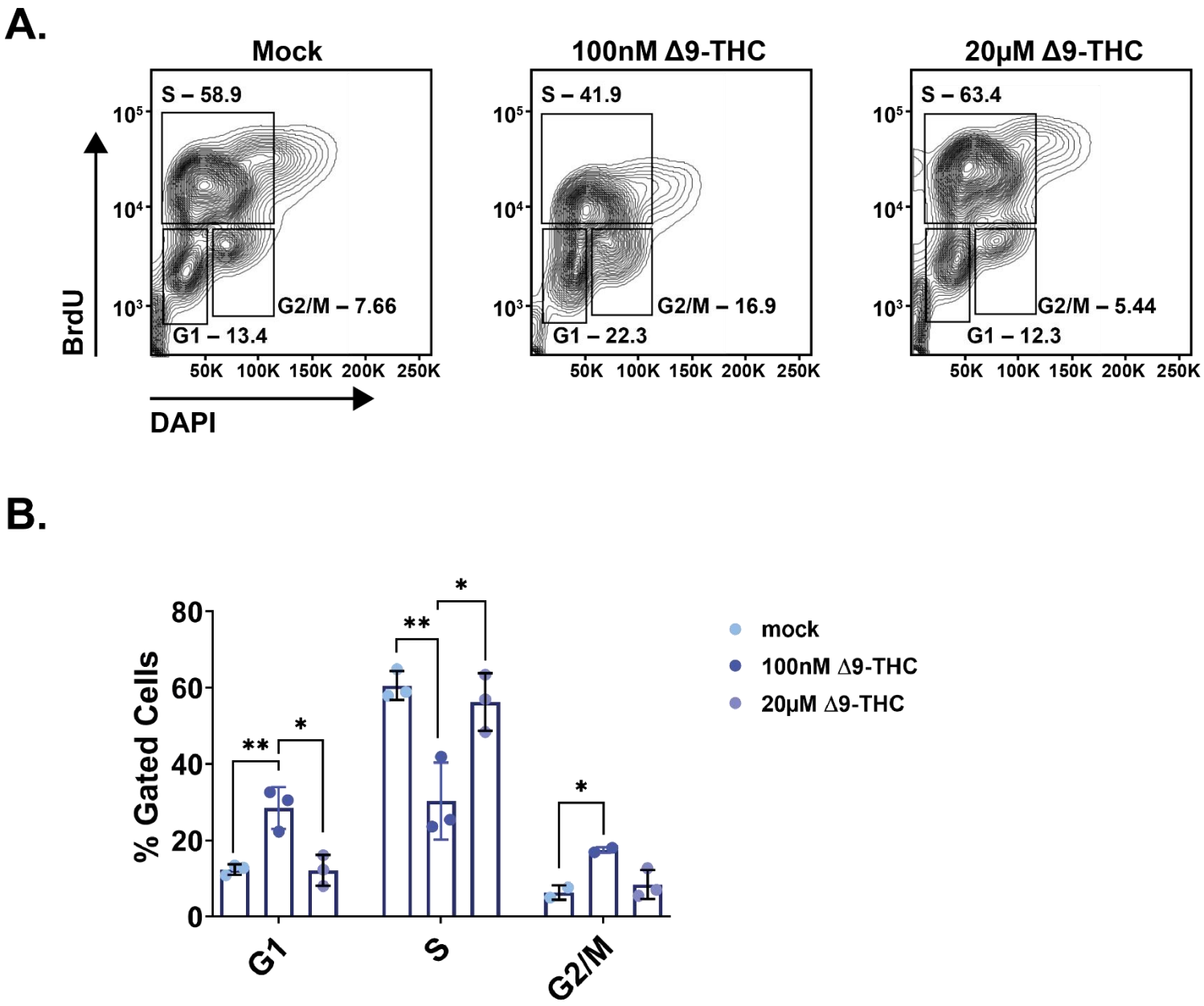

1096 **Supplementary Figure 3**

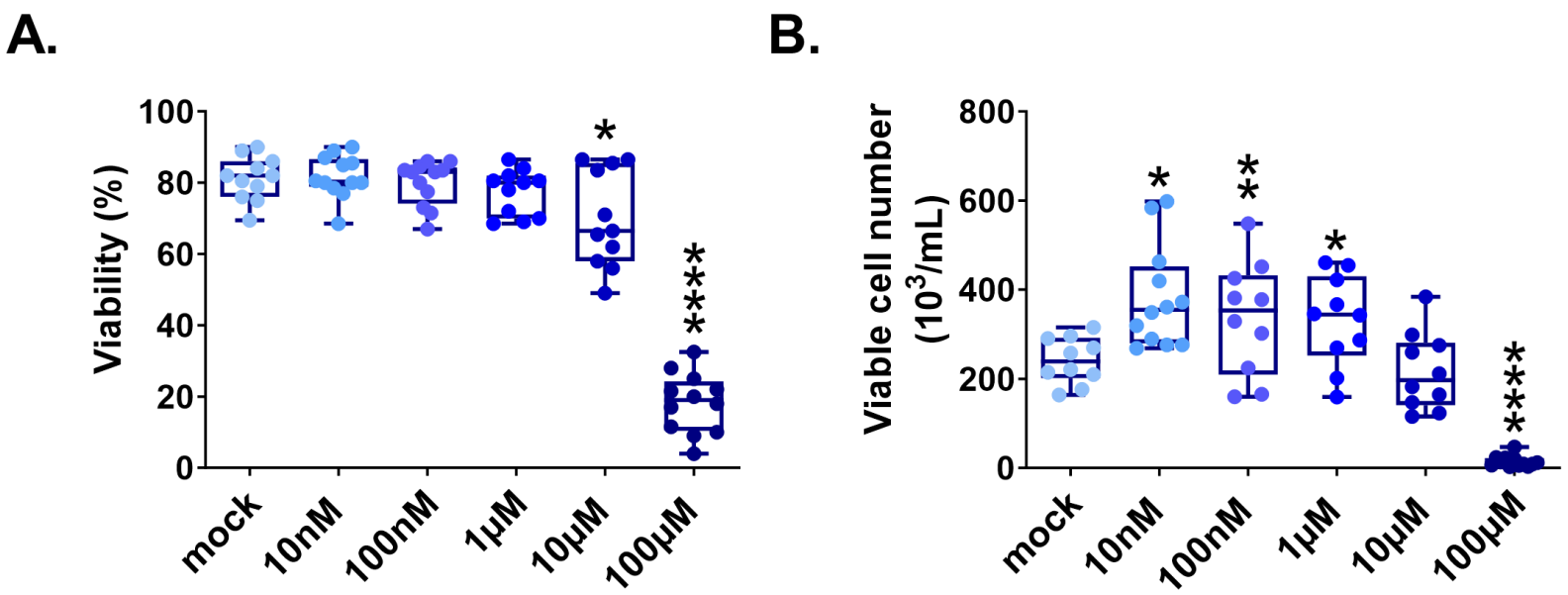

Supplementary Figure 4

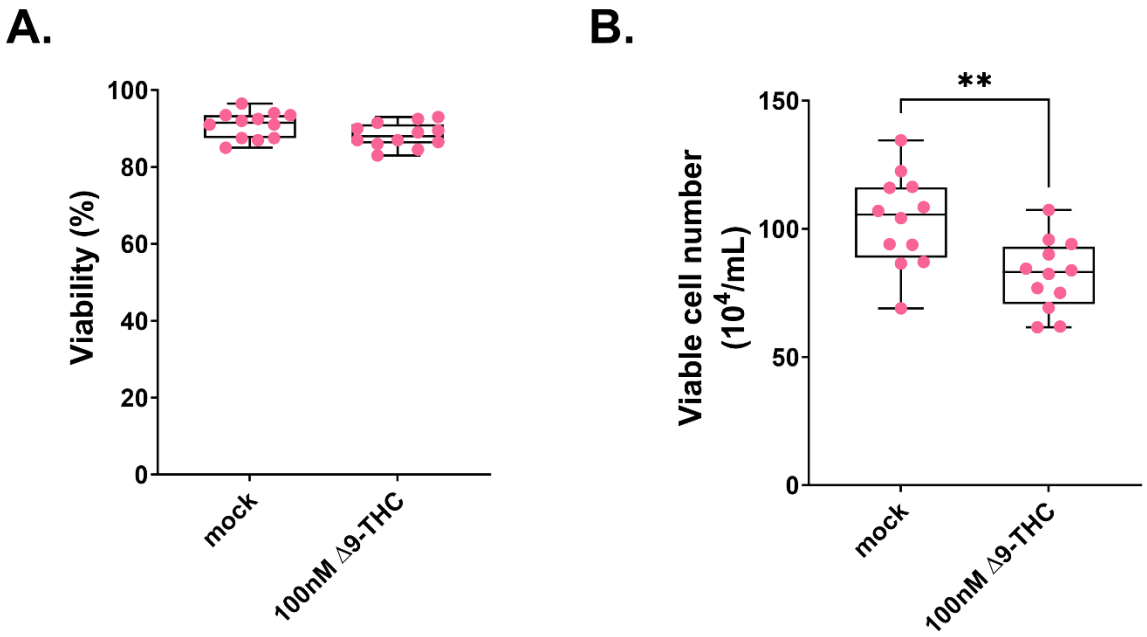

Supplementary Figure 5

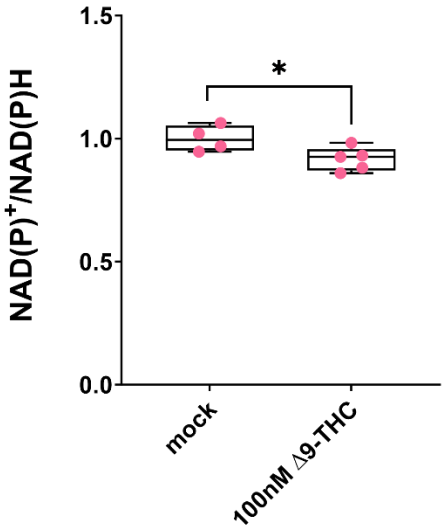

Supplementary Figure 6

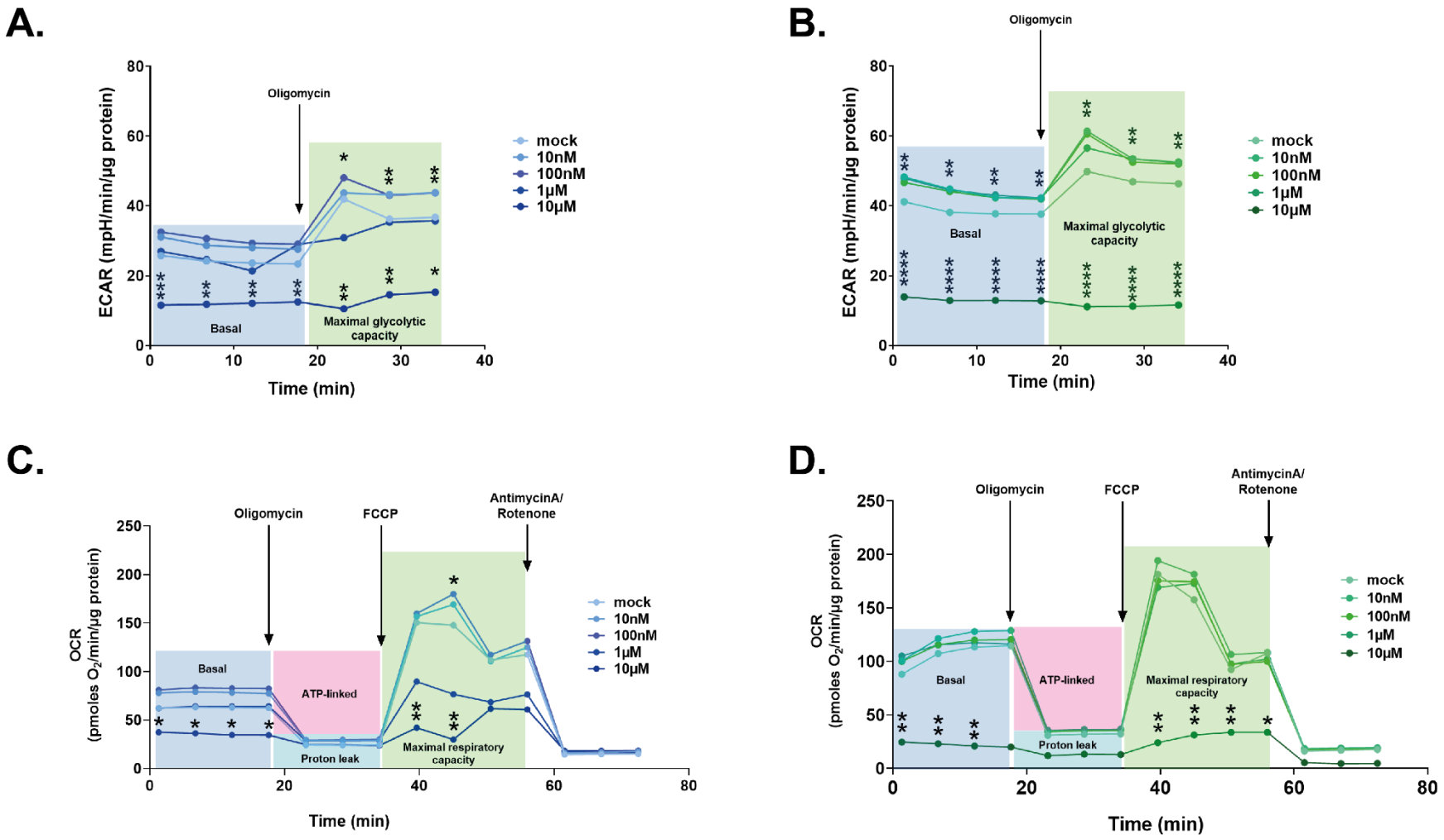

Supplementary Figure 7

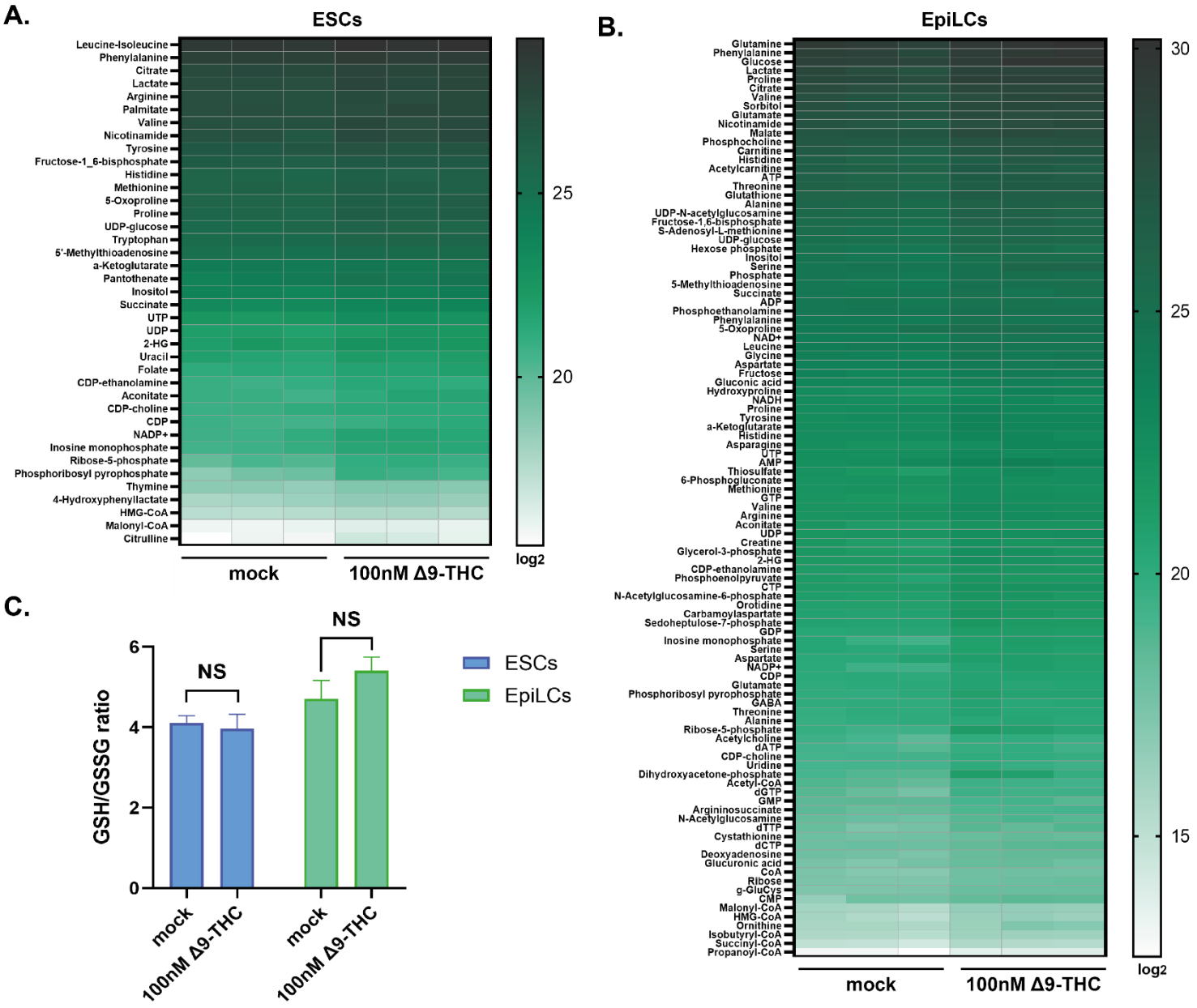

Supplementary Figure 8

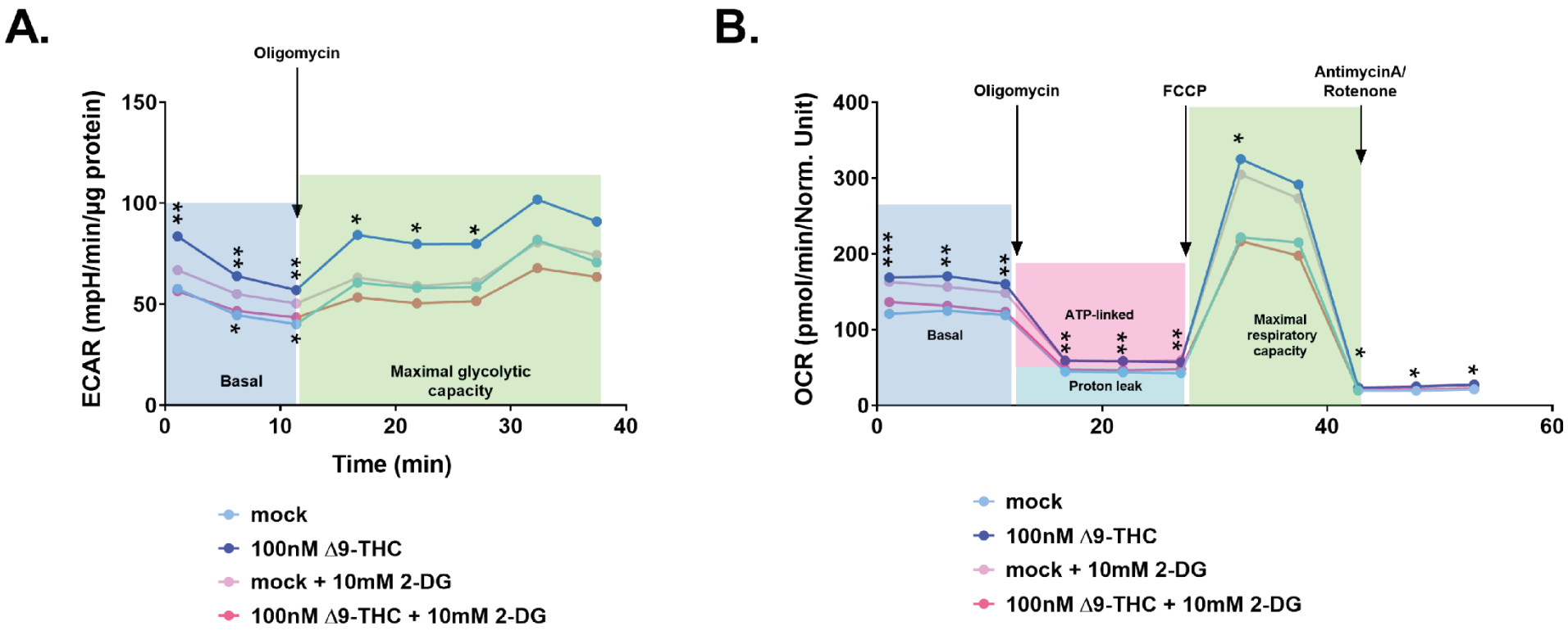

Supplementary Figure 9

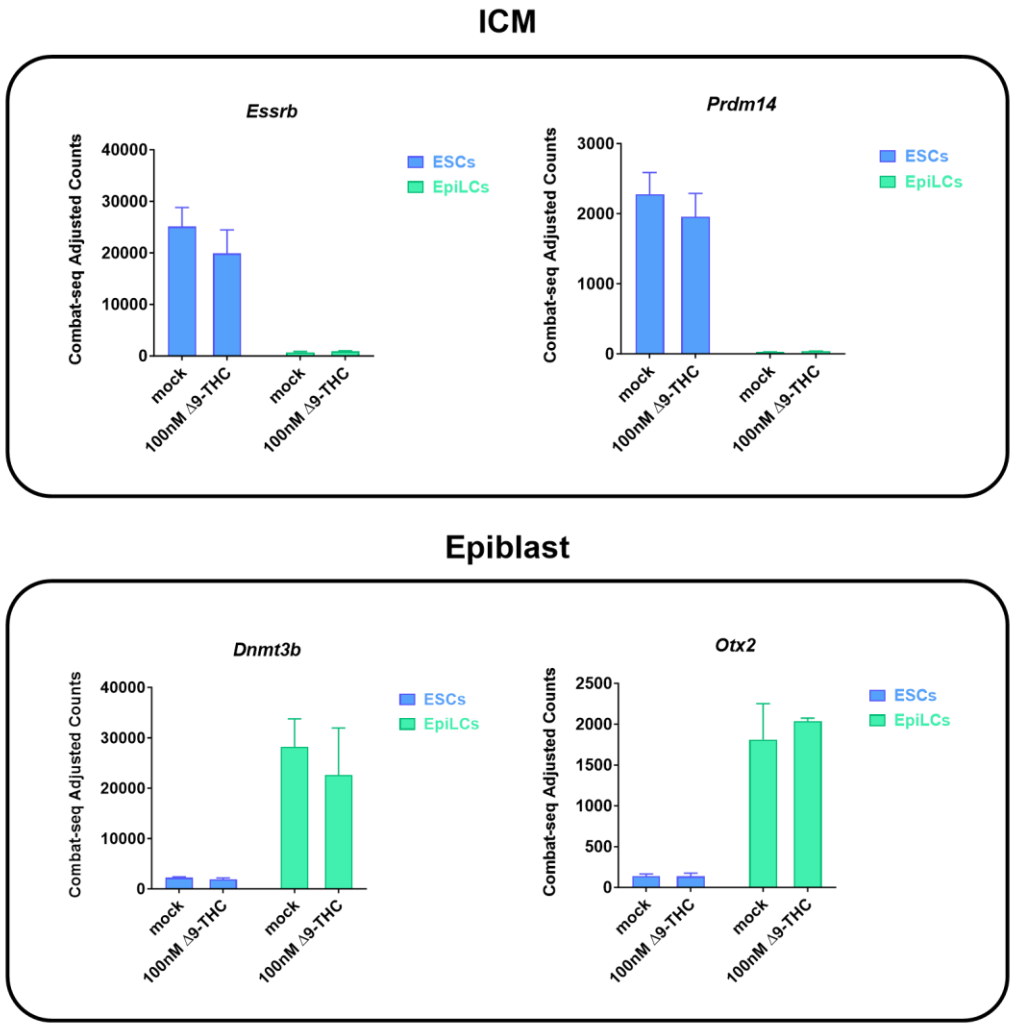

Supplementary Figure 10

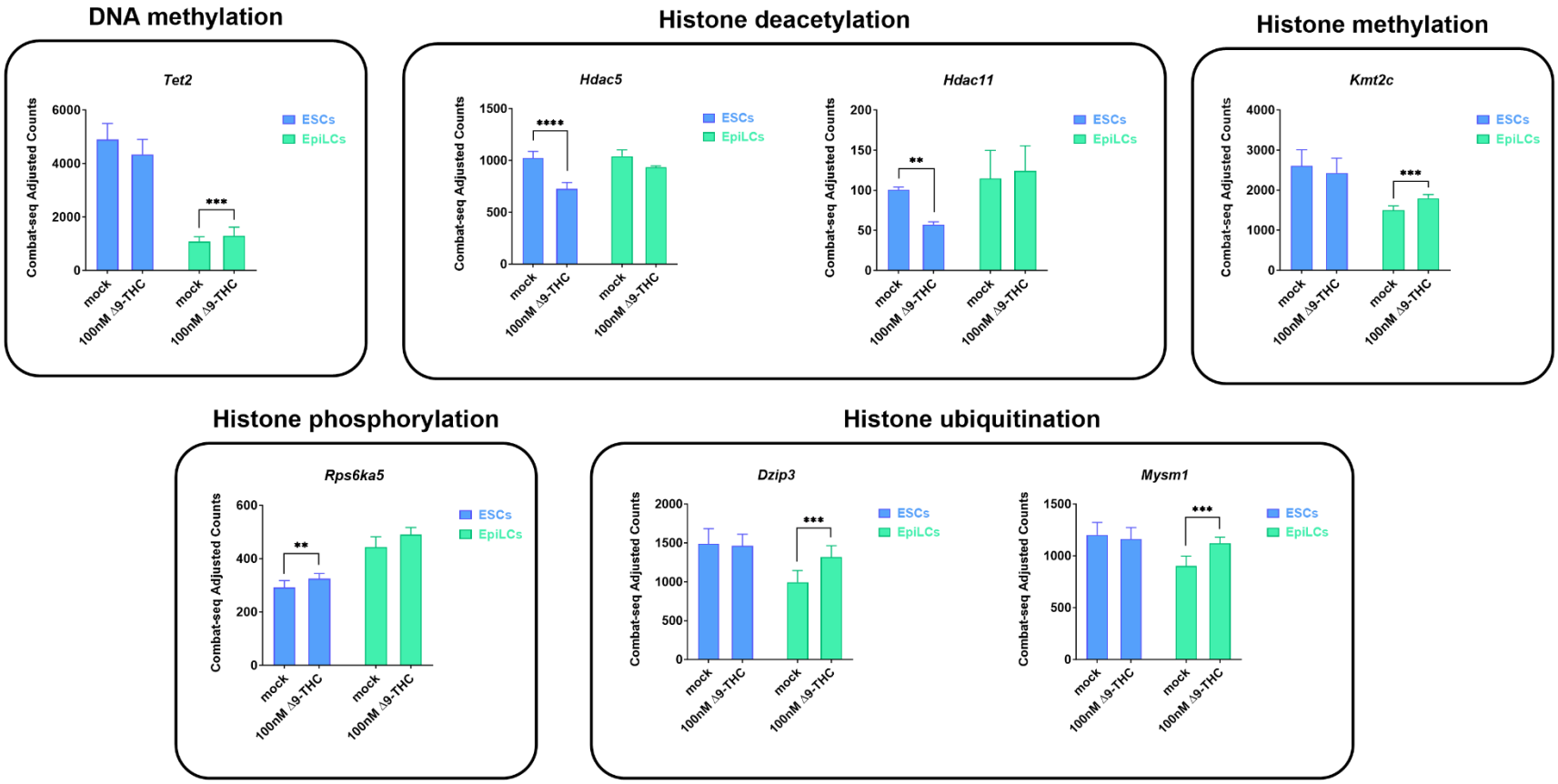

Supplementary Figure 11

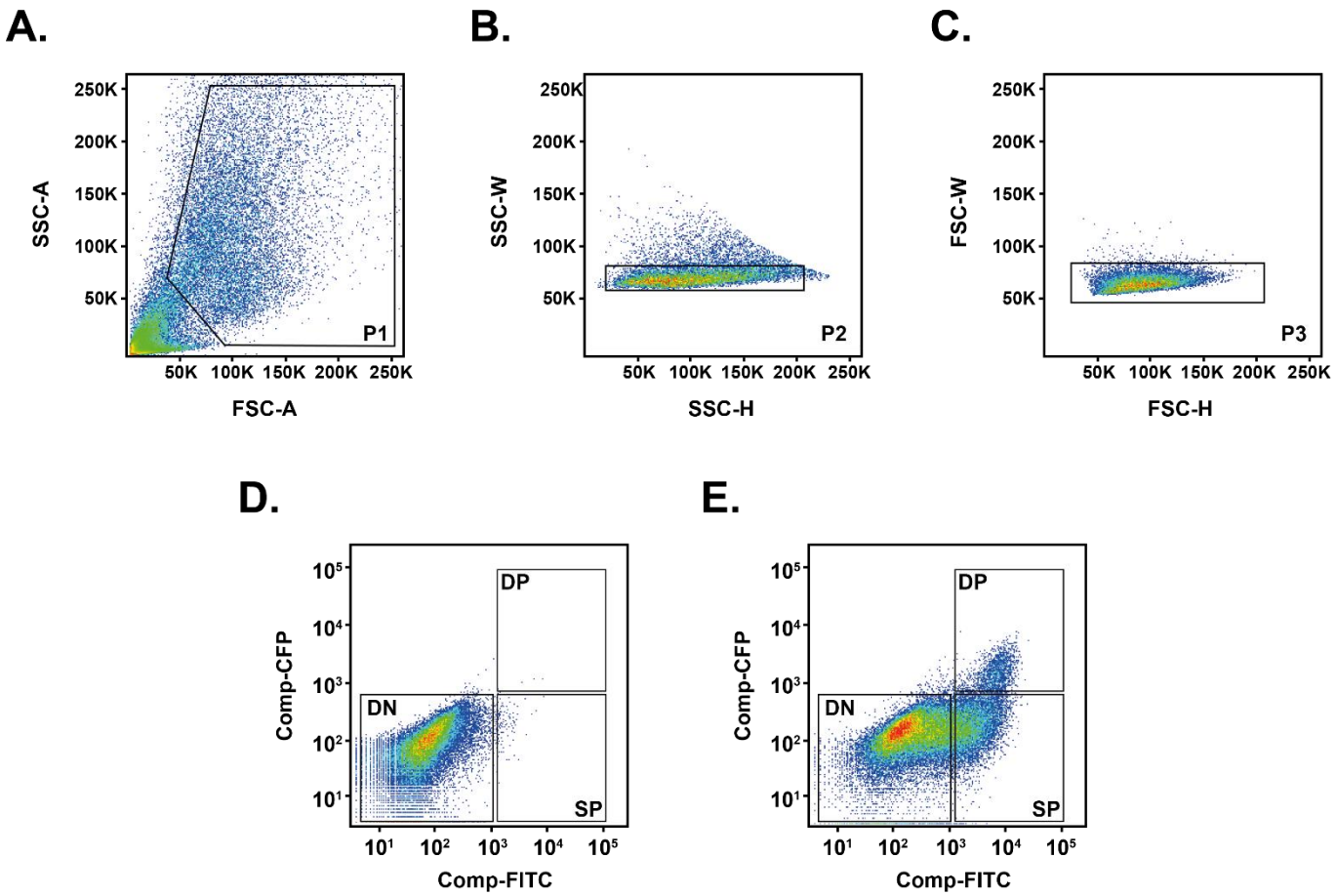

Supplementary Figure 12

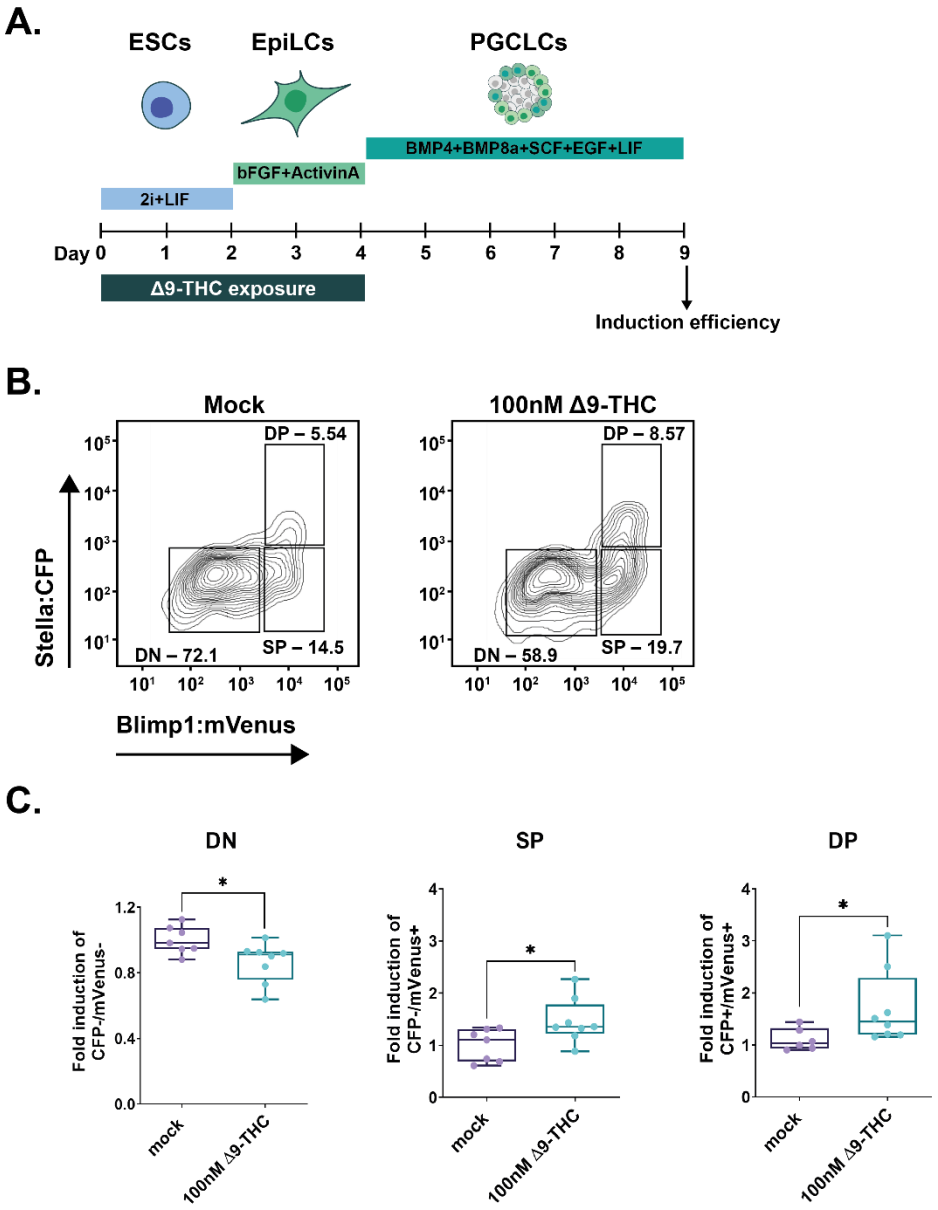

Supplementary Figure 13